frontiers | Frontiers in Earth Science

ORIGINAL RESEARCH
published: 27 May 2022
doi: 10.3389/feart.2022.906949

Evaluation of the Effectiveness and Adaptability of a Composite Water Control Process for Horizontal Wells in Deepwater Gas Reservoirs

Dianju Wang[1,2,3]*, *Yihe Li*[4], *Lan Ma*[5], *Fahao Yu*[6], *Shufen Liu*[4], *Tong Qi*[1] and *Siyuan Jiang*[1]

[1]Heilongjiang Key Laboratory of Gas Hydrate Efficient Development, Daqing, China, [2]College of Offshore Oil and Gas Engineering, Northeast Petroleum University, Daqing, China, [3]Sanya Offshore Oil and Gas Research Institute, Northeast Petroleum University, Sanya, China, [4]College of Earth Science, Northeast Petroleum University, Daqing, China, [5]Northeast Petroleum University Qinhuangdao, Northeast Petroleum University, Qinhuangdao, China, [6]Bohai Oilfield Research Institute of CNOOC Ltd., Tianjin, China

OPEN ACCESS

Edited by:
Jinze Xu,
University of Calgary, Canada

Reviewed by:
Jun Zhou,
Southwest Petroleum University, China
Zhiyuan Wang,
China University of Petroleum, Huadong, China
Li Zhonghui,
Yangtze University, China

***Correspondence:**
Dianju Wang
djwang@nepu.edu.cn

Specialty section:
This article was submitted to Environmental Informatics and Remote Sensing, a section of the journal Frontiers in Earth Science

Received: 29 March 2022
Accepted: 08 April 2022
Published: 27 May 2022

Citation:
Wang D, Li Y, Ma L, Yu F, Liu S, Qi T and Jiang S (2022) Evaluation of the Effectiveness and Adaptability of a Composite Water Control Process for Horizontal Wells in Deepwater Gas Reservoirs. Front. Earth Sci. 10:906949. doi: 10.3389/feart.2022.906949

Deepwater gas fields have high bottom water energy and a high risk of seeing water. Higher requirements are put forward for the water control process to control the water effect. This article is based on the actual background and well design of the X gas field in the South China Sea and on three sets of physical simulation experiments and three sets of numerical simulation experiments. An analysis and comparison of the water control effect of a combination of continuous packer, continuous packer and variable density screen tube, and their adaptability evaluation in deepwater gas reservoirs were performed. The results obtained from the numerical and physical simulations are consistent. The experimental results show that the water control process of a continuous packer is mainly based on the water-seeing and water-blocking ability. It is less capable of extending the time to produce water in the horizontal section. However, its water-blocking ability is strong and is able to seal the water spot quickly. It extends the total production time by 12.29% and increases the total gas production by 5.96%; the combined water control process of the continuous packer and variable density screen tube can effectively play their respective advantages of water control. The combination of the continuous packer and variable density screen tube can effectively be advantageous of their respective water control processes, enabling the gas–water interface to advance in a balanced manner, extending the water-free gas recovery period by 11.61%, extending the total gas production time by 15.76%, and increasing the total gas production volume by 13.75%. Both water control processes have good applicability in deepwater gas fields and have certain sand control capability. It is conducive to the one-time completion operation for the commissioning of deepwater gas fields.

Keywords: deepwater gas field, water control process, continuous packer, variable density screen tube, physical simulation

INTRODUCTION

As China's gas reservoir exploration and development in the Southeast Qiongdongnan Basin moves toward deeper water, some of the reservoirs are experiencing difficulty in moving water reserves (Chen et al., 2020). This is especially true in terms of gas reservoir production seeing water. The Lingshui 25–1 gas field, for example, faces a water depth of nearly 1,000 m. The design well depth is nearly 4,000 m, the pressure coefficient of the target layer is 1.7–1.9, and the temperature reaches 150°C. In the gas reservoir production environment (Shi, 2015), there are challenges of high bottom water multiples and high energy (Chen et al., 2020). These place higher demands on the water control process and its effectiveness during extraction. By increasing the contact area between the wellbore and the reservoir, the production capacity can be effectively increased. Especially in deepwater gas reservoirs, horizontal wells have become the main production well type. However, the problem of excessive water production has also become more prominent (Sun and Bai, 2017). At present, domestic and foreign horizontal well water control processes are widely used mainly in oil reservoirs. The compressibility of natural gas allows it to be extracted at a higher seepage rate than oil wells, and water intrusion poses a greater risk to gas reservoir development than to oil reservoir development (Xu et al., 2018; Xu et al., 2021).The ability of horizontal wells to produce gas rapidly decreases or even stops when water is present. As a result, the implementation of simple "drainage" and "plugging" water control techniques at a later stage is limited (Wang et al., 2001). A combination of pre- and post-water control techniques needs to be applied. Therefore, there is still much room for exploration of water control techniques for gas reservoirs and their effective implementation. A great deal of research and experimentation has been carried out on water control techniques for horizontal wells. However, they have mainly been applied to oil reservoirs. Considering the high temperature and high pressure production background and characteristics of deepwater gas reservoirs, in this study, it is concluded that both the variable density screen tube and continuous packer water control processes have good water control effects in gas reservoirs.

The principle of the variable density screen tube water control process is to compare the non-homogeneity of the producing formation in horizontal wells. Changing the horizontal well borehole density effectively delays the bottom water or gas top cone entry time in horizontal wells (Zhou, 2007; Pang et al., 2012). Horizontal wells use a low borehole density in the high-permeability section of the producing formation to reduce the rate of inflow at this location. High-density boreholes are used in the low-permeability section of the formation to increase the rate of inflow at this location, equalising the rate of bottom water rise throughout the horizontal section and preventing early cone in of bottom water and see water (Zhou, 2007; Wei et al., 2009; Li et al., 2010). Due to the limitations of the process technology, it is not possible to achieve a completely uniform inflow profile by varying the density of the orifice (Xu et al., 2019; Xu et al., 2020). Hence, it is necessary to improve this by staging different density orifices (Sun et al., 2011). However, the effectiveness of segmented variable density water control is guaranteed by the requirement that the different sections of the borehole have the desired inflow velocity (Wei et al., 2009). Therefore, this requires that in practice, a packer is placed between each section to achieve out-of-tube containment. The packers have high sealing capacity and stability (Rao et al., 2010). However, the high temperature and pressure conditions in deepwater gas reservoirs place higher demands on the packers used in horizontal well section completions (Zhao et al., 2012). In addition, considering that non-uniform flow of crude oil is due to reservoir non-homogeneity and frictional pressure drop along the wellbore, one practical way to reduce this problem is to use inflow control devices between packers by adjusting the inflow and distribution of production within each isolated section (Sun et al., 2011; Wang et al., 2011; Irani et al., 2021). However, the device itself and the packers used in conjunction with it need to meet both high-temperature and high-pressure conditions.

The principle of the AICD flow regulating screen tube water control process in oil reservoirs is based on the difference in viscosity coefficients of oil and water. The different effects of fluid inertia forces and viscous resistance are used to control the discs to achieve water flow inhibition (Yan et al., 2021). This mitigates the "heel–toe effect", leading to an uneven inflow of crude oil at the "heel" and "toe" ends of the horizontal well, resulting in an uneven cone of bottom water (Zeng et al., 2014). Oil is more viscous than water, but gas is less viscous than water. This opposite viscosity class causes AICD to be non-applicable for gas field applications. The nozzle-type ICD controls the fluid velocity in the horizontal section to maintain uniformity by adjusting the nozzle size and density. It has achieved good water control and oil enhancement results in offshore oil fields. However, its anti-clogging performance and anti-flushing performance make it difficult for its application in high production gas wells. The continuous packer is the annulus between the well wall and the screen tube filled with fine coated polymer granular gravel. The film on the surface increases the resistance to the axial flow of the fluid in the annulus and acts as a barrier to water movement in the annulus. This is similar to the presence of a bare eye external packer between each screen tube, which has the effect of continuously preventing water from entering the horizontal section. The water-blocking, breathable cladding is now fully compatible with high-temperature, high-pressure gas reservoir production environments (Liu et al., 2020). This combination significantly reduces the fugitive flow of produced fluids in the outer annulus by filling the naked eye annulus with lightweight particles. In combination with the downstream ICD/AICD, it reduces the production pressure differential in the high-permeability water-seeing layer and increases the production pressure differential in the low-permeability oil-producing layer, which enables subdivision of the entire well section to regulate the flow and control water (Wan et al., 2020; Yan et al., 2021; Zhang et al., 2021). However, in deepwater reservoirs, the density and viscosity of natural gas are less than those of water. Therefore, ICD/AICD screen tubing cannot be used to produce gas and control water in

TABLE 1 | Main relevant parameters for numerical simulation experiments.

Gas reservoirs		Horizontal wells	
Initial pressure (Mpa)	43.3	Length of the horizontal production section (m)	580
Gas reservoir thickness (m)	20	Inner diameter of the screen tube (m)	0.1491
Gas density (kg/m^3)	0.65	Single-hole diameter of the screen tube (m)	0.01
Gas viscosity (mPa-s)	0.045	Maximum hole density (holes/m)	300
Volume factor (10^{-3} m^3/m^3)	3.5	Reasonable gas extraction rate (%)	3.5–4.0
Average porosity	0.2	Daily gas production (10^4 m^3/d)	50
Bottom water multiplier	100	Height of water avoidance (m)	59.1
Average permeability (mD)	13.7	Well control area (cm^2)	4.9×10^9

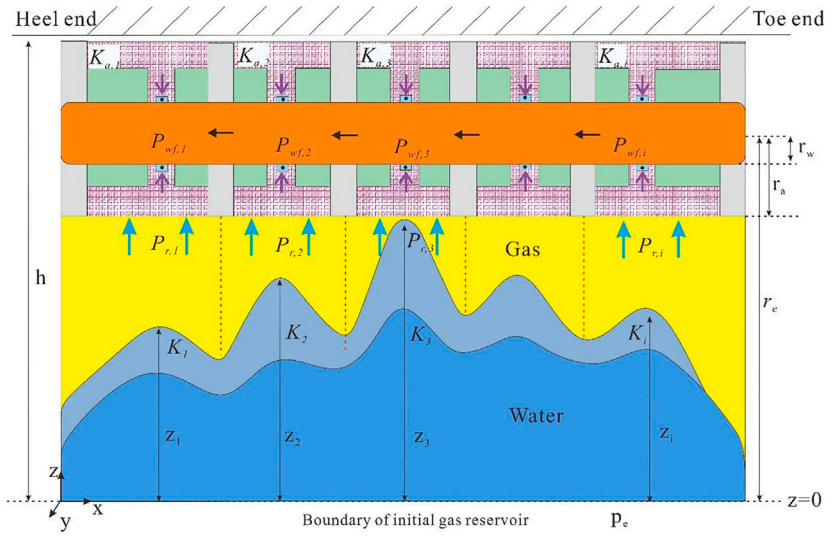

FIGURE 1 | Compound water control process production pressure drop model.

gas reservoirs. The ICD/AICD is a passive device, and once it is placed in the completion tubing column, it cannot be adjusted during production to ensure flow equalization (Sun et al., 2011).

In response to the abovementioned problems with the water control process, this study considers the advantage of continuous packers to mitigate fluid cascading in the annulus outside the pipe. It can effectively enhance the coincidence of the gas production rate and reservoir inhomogeneity at different locations of the variable density screen tube. By combining the advantages of the two water control processes, a water control process combining a variable density screen tube and a continuous packer is designed. The water control effect of this combination in deepwater gas reservoirs is also evaluated by combining physical and numerical simulation methods.

MATHEMATICAL MODEL

Model-Related Parameters

The H1 well is a designed well location for the Nanhai X gas reservoir, with bare-hole completion and gravel-filled sand control. The gas reservoir temperature is approximately 128°C, the reservoir pressure is nearly 40 MPa, the bottom water multiple is 100 times, the height of water avoidance in the horizontal section is 59.1m, the horizontal section length of the design is 580 m, and the screen tube diameter is approximately 15 cm (**Table 1**).

Mathematical Models

Considering the H1 well is a bare-borehole completion, continuous packer technology allows for an "infinite section" completion. Flow control was applied to each section by separately modeling the pressure and pressure drop distribution in the horizontal section. The analysis of the effect of different water control processes on the evolution of the gas–water interface under constant production conditions was carried out. The gas reservoir seepage model was readjusted to consider the higher percolation rates of natural gas during the extraction of the gas reservoir. The model was adjusted to better match the parameters of the water control process (**Figure 1**).

It is assumed that each section of the horizontal well flows in a continuous packer plane radially; the gas reservoir is

bottom water–bounded and the fluid conforms to the Darcy flow law.

$$q_r = \frac{2\pi rhk}{\mu}\frac{dp}{dr}. \tag{1}$$

According to the continuity equation, it follows that

$$\rho q = \rho_1 q_1 = \rho_2 q_2 = \text{constant}. \tag{2}$$

Joint compression factor gas equation of state

$$\rho = \frac{pM}{ZRT}. \tag{3}$$

The flow at the radius r can be converted to the standard state flow at $q_r q'_r$

$$q_r = q'_r B_g = q'_r \frac{p_{sc}}{Z_{sc}T_{sc}}\frac{ZT}{p}. \tag{4}$$

Separating the variables yields

$$\frac{2\pi KhT_{sc}Z_{sc}}{q'_r p_{sc} T\mu Z} pdp = \frac{dr}{r}. \tag{5}$$

For steady-state flow, the outer boundary pressure is constant and the mass flow rate in each horizontal section of the packer is constant. Then, there is

$$\frac{774.6Kh}{q_{sc}T} 2\int_{pwf}^{p} \frac{p}{\mu Z} dp = \ln\frac{r}{r_w}. \tag{6}$$

The aforementioned equation can be converted to

$$\frac{p}{\mu Z} = f(p). \tag{7}$$

Using the concept of anthropomorphic pressure, there is

$$\psi = 2\int_{p0}^{p} \frac{p}{\mu Z} dp. \tag{8}$$

Applying the mean pressure equation is equivalent to

$$q_{sc} = \frac{774.6Kh\left(p_e^2 - p_{wf}^2\right)}{T\bar{\mu}\bar{Z}In\frac{r_e}{r_w}}. \tag{9}$$

$$p_e^2 - p_{wf}^2 = \frac{1.291\times10^{-3} q_{sc}T\bar{\mu}\bar{Z}}{Kh} In\frac{r_e}{r_w}. \tag{10}$$

According to the Hawkins equation, the epidermal coefficient is expressed as

$$S = \left(\frac{K}{K_a} - 1\right)\ln\frac{r_a}{r_w}. \tag{11}$$

When Ka < K, the additional pressure drop is greater than 0; then, we have

$$\Delta p_{skin}^2 = \frac{1.291\times10^{-3} q_{sc}T\bar{\mu}\bar{Z}}{Kh} S. \tag{12}$$

$$p_e^2 - p_{wf}^2 = \frac{1.291\times10^{-3} q_{sc}T\bar{\mu}\bar{Z}}{Kh}\left(In\frac{r_e}{r_w} + S'\right). \tag{13}$$

Combining the pressure drop from the epidermal effect into the total pressure drop, the stable flow Darcy capacity equation is

$$q_{sc} = \frac{774.6Kh\left(p_e^2 - p_{wf}^2\right)}{T\bar{\mu}\bar{Z}\left(In\frac{r_e}{r_w} + S\right)}. \tag{14}$$

$$p_e^2 - p_{wf}^2 = \frac{1.291\times10^{-3} q_{sc}T\bar{\mu}\bar{Z}}{Kh}\left(In\frac{r_e}{r_w} + S\right). \tag{15}$$

According to the distribution characteristics of the permeability size of the horizontal section of the horizontal well, it was mainly divided into five sections. The distance of each section from the location of the heel end is 0–33 m, 33–178, 178–307, 307–358, and 358–580, and the numerical model determines that the average permeability of the formation in the near horizontal section of the well is 23.5 mD, that is, 0.0232 μm2. Combined with the analysis of the coefficient of variation of the permeability of the near well, that is,

$$C = \sqrt{\frac{1}{n}\sum_{i=1}^{n}\left(k_i - \bar{k}\right)^2}\Big/\bar{k}, \tag{16}$$

where k_i is the near-well permeability of the micro-element of the wellbore in section i, m^2 and $\bar{k}$ is the average permeability of the near-well, m^2. Based on the characteristics of the permeability distribution of the six sections of the horizontal section reservoir, the permeability distribution of each section was more homogenous. Therefore, this analysis will be approximated as six horizontal section microelements to obtain the coefficient of variation between each section of the near analysis. The coefficient of variation for the horizontal section of well H1 was calculated to be 0.4 (**Table 2**, **Figure 1**). We believe that the production profile can be improved by optimizing the pore density, but there are fluctuations (Wang et al., 2012). The optimization of the sieve tube borehole density in this study was carried out based on the horizontal well shot hole optimization model (Wang et al., 2012). By setting the flow rate distribution in the horizontal section to the equilibrium state, a system of equations with borehole density as the decision variable is solved. Initially, the screen tube hole densities of the six horizontal section microelements were determined to be 51holes/m, 263holes/m, 62holes/m, 300holes/m, 44holes/m (**Table 2**).

PHYSICAL SIMULATION EXPERIMENTS

Experimental Setup and Procedure

The interior of this experimental setup is a 50 cm × 50 cm × 50 cm square kettle (**Figure 2**). The 100 water saturation measurement sensors inside the kettle and 20 pressure sensors are evenly distributed throughout the chamber. According to the target gas reservoir conditions, air was used instead of natural gas and distilled water instead of experimental bottom water during the experiments. There was one gas injection valve at the top of the kettle. The gas reservoir bottom water multiplier was large and vigorous. In order to simulate the ability of the bottom water to cone in at the horizontal section position during gas reservoir production, three inlet valves were installed at the bottom of the unit. The valves were connected to uniformly open water injection pipes. The kettle was recharged by an ISCO pump

TABLE 2 | Horizontal sieve pipe section segments and shot hole density.

Penetration segment	Length interval (m)	Penetration rate		Average permeability of near wells		Coefficient of variation	Sieve tube hole density
		mD	μm²	mD	μm²		pcs/m
First paragraph	0–33	30	0.03	23.5	0.0232	0.4	51
Second paragraph	33–178	12	0.012				263
Third paragraph	178–307	28	0.028				62
Paragraph 4	307–358	10	0.01				300
Paragraph 5	358–580	31	0.03				44

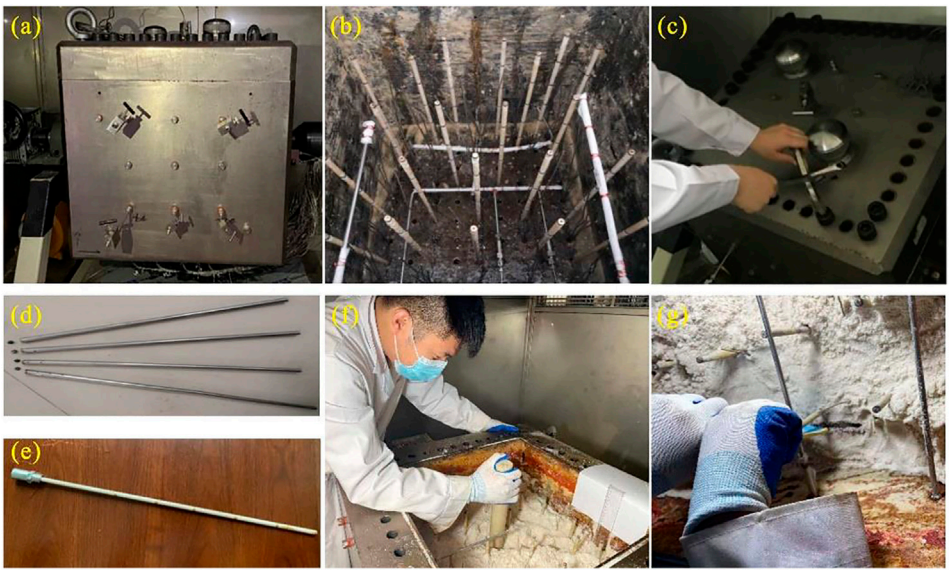

FIGURE 2 | Physical simulation equipment for water control processes. **(A)** kettle body; **(B)** measuring points and laying inside the equipment; **(C)** kettle body sealing; **(D)** sieve tube; **(E)** measuring points; **(F)** sand compaction in sections; **(G)** sand sampling.

at constant pressure, and a panel with uniform openings was installed above the three water injection pipes to create a bottom water layer by "surface injection" instead of "spot injection." The balanced injection design prevents the effect of injection operation on the bottom water cone. A small condensing unit was added to the middle of the gas extraction pipe, and the lower part of the unit was connected to a water collection device. A gas flow meter was connected at the end of the gas extraction pipe to determine the rate of gas extraction and count the volume of gas extracted.

Based on the different phases of the physical simulation experiment, the overall procedure was divided into three processes: initial model building, simulation of the water-free gas extraction period, and simulation of the water-seeing period and production shutdown.

1) Initial model building includes sand filling, sand segment compaction, horizontal segment laying, kettle sealing, gas and water injection equipment connection, and gas–water interface building. In particular, the gas–water interface was established considering that the actual reservoir had 23% bound water saturation formation. Therefore, a full model sand body with 100% water content was used to replace the upper aquifer by top pressure gas injection through the kettle body. This was carried out until the formation was 23% saturated with bound water. The final gas–water interface was determined after the criteria were adjusted by cyclic water and gas injection. A stable gas–water interface was obtained for the entire experimental setup for 12 h. That is, the gas–water saturation field of the entire model no longer changes significantly. At this point, the water avoidance height conforms to the geometric model settings.
2) Gas reservoir extraction simulation—The gas production valve of the horizontal well was opened and the gas recovery rate was set to a reasonable recovery rate. The gas recovery situation and total gas recovery volume every 1 h were recorded and the gas recovery rate was calculated. The characteristics of gas and water distribution at different section locations at each time are recorded through 3D visualization software. When the extraction channel began

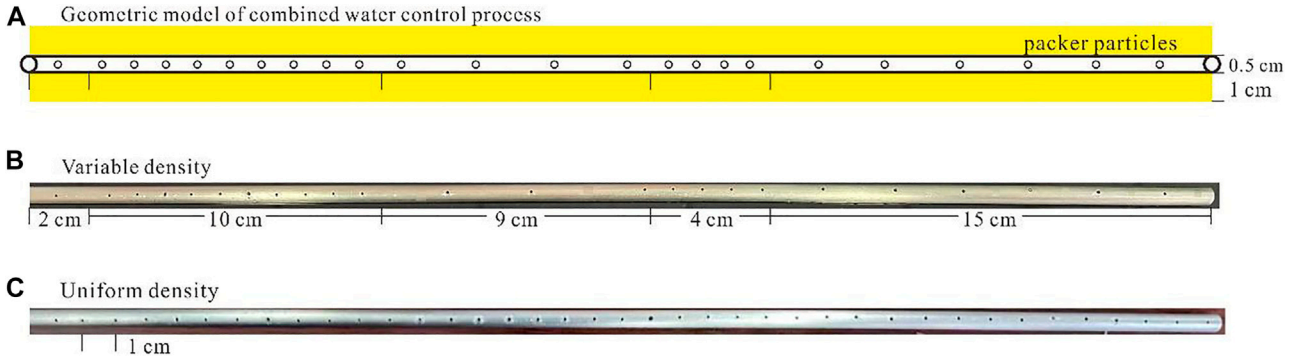

FIGURE 3 | Composite water control process geometry model and screen tube design. **(A)** Geometric model of combined water control process. **(B)** Variable density, and **(C)** uniform density.

TABLE 3 | Table of H1 well segmentation and physical model parameter design.

Horizontal segment/cm	0–2	2–12	12–21	21–25	25–40
Reservoir segmental permeability/mD	30	12	28	10	31
Model segmental permeability/mD	300	120	280	100	310
Uniform density eyelets (pcs/cm)	1	1	1	1	1
Variable density eyelets (pcs/cm)	0.5	0.9	0.44	1	0.4

to produce water, the production time and gas-water saturation field were recorded, and the gas–water interface and the location of water production at this time were determined. Total water production was collected and recorded until the gas well stopped producing.

3) The gas well was shut down, and the experiment was completed. The standard for gas well shutdown was when the water content reached 98%. The gas production valve was closed and the experimental data were collated. The total production time, total gas production, and gas–water saturation field were recorded, focusing on completing the characterization of the distribution of water bodies in the horizontal section location.

Experimental Model Design

The geometric model of the physical simulation experiment was designed with a gas–water interface height of 20 cm and a water avoidance height of 20 cm. The horizontal well section was located in the middle position of the kettle. The length was 40 cm, internal diameter 0.5 cm, and borehole diameter 0.1 cm (**Figure 3**). The model stratigraphic setting was completed by filling with sand and compacting. Reservoir construction was based on the permeability distribution characteristics of the horizontal section trajectory of the H1 horizontal well. That is, a non-homogenous reservoir with five permeability stages. In order to effectively enhance the vertical segmentation characteristics of the reservoir, the kettle was divided into five separate spaces by combining four thin steel plates with sieve holes embedded in the joints of each section of the formation. Each separate space was filled and compacted with quartz sand of different mesh sizes. This was used to simulate water intrusion in a non-homogenous gas reservoir. The sand model was completed by mechanical compaction. The reservoir permeability of each section of the sand-filled model was equated with the corresponding core at a ratio of 10:1. The non-homogenous character of the original formation was ensured (**Table 3**). This process was achieved by repeated sampling and testing with a core hole and percolation tester until the permeability ratio between the two on the core scale was met.

The physical experiments were divided into three groups: the no water control process experiments, the continuous packer water control process, and the combined variable density sieve tube and continuous packer process experiments. The pore density of the production screen without the water control process model and continuous packer water control process model is of uniform density, that is, 1/cm (**Figure 3C**, **Table 3**). The variable screen tube pore density was calculated based on the permeability of different reservoir sections (**Table 3**). Both the continuous packer water control process model and the combined water control process model were lined with laminated packer particles at the screen tube and bare eye annulus. Based on the experiments, it was found that the filling thickness of the laminated particles had a significant effect on the effective additional resistance generated by the particles themselves. The greater the filling thickness, the greater the additional pressure drop. Thus, a large lateral filling thickness can effectively reduce the lateral gas fugacity. Based on the results of the analysis of the additional pressure drop generated by the thickness of the clad gravel, a thickness of 1 cm was set for this physical simulation experiment (**Figure 3**, **Figure 4**). Finally, the results of the simulations on the effect of different water control processes on the water intrusion profile characteristics, time to water production, and the final total production were used to complete the evaluation of the suitability of water control processes in gas reservoirs.

With the assurance that the model and the formation use the same pore medium and that the fluid density and viscosity are constant, if the two similar criteria of the ratio of the gravity and driving forces of the gas and water phases are to be satisfied, the gas recovery rate ratio will be the square of the length ratio (Shen et al., 2013). The experimental model was scaled down to 103:1 based on the actual parameters of well H1. From the similarity criterion, the gas recovery rate was the square of the length ratio, that is, 106:1. The

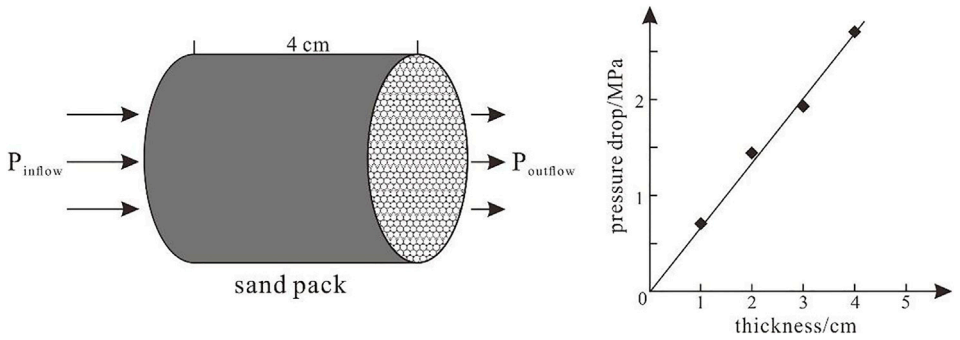

FIGURE 4 | Pressure drop test results from filling thickness on gas flow.

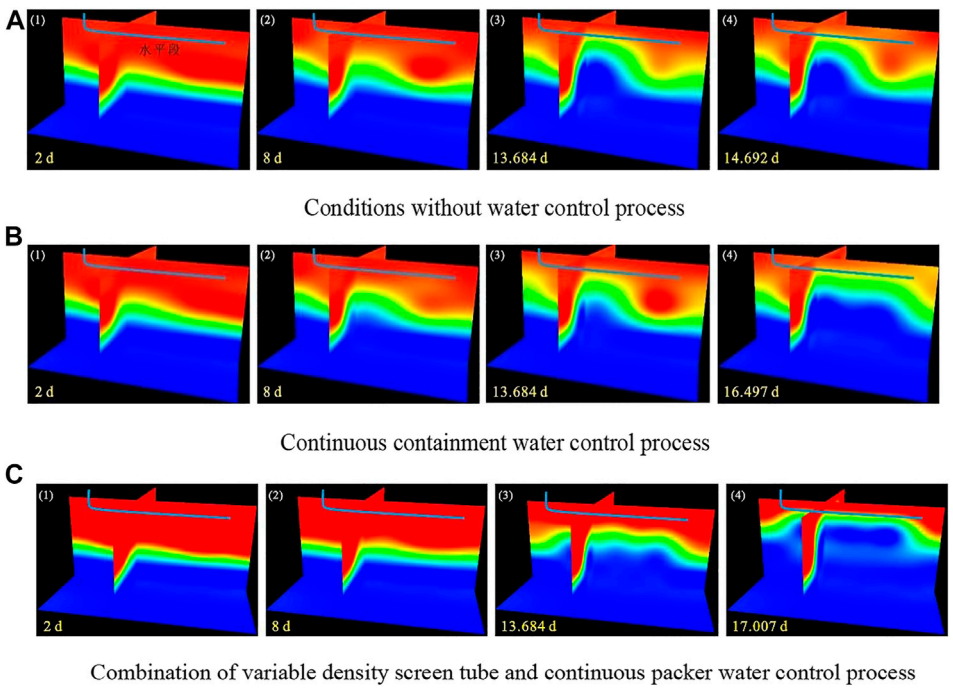

FIGURE 5 | Evolution of the gas–water saturation field under different water control measures. **(A)** Conditions without water control process. **(B)** Continuous containment water control process. **(C)** Combination of variable density screen tube and continuous packer water control process.

equivalent gas recovery rate for the physical model was thus calculated to be approximately 200 L/d. The reactor volume was 100 L, the average porosity after sand compaction was 22.4%, and the height of the water body in the reactor was 20 cm, so the space occupied by gas was approximately 16.8 L. The ideal gas state equation calculated the gas reservoir environment to be 43.3 MPa. The volume of gas filling in the kettle at ambient temperature and pressure was approximately 5379 L. This met the reasonable gas recovery rate setting for well H1 (**Table 1**).

Physical Simulation Results

Model 1 was an experiment model without water control measures. Based on the gas–water saturation evolution, the results show that as production progresses, the bottom water starts to cone in from the middle of the horizontal section and finally water is produced in the middle of the horizontal section (**Figure 5A**). Model 1 gas production began to show water at 13.684 days. When gas production reached 14.692 days, the water content reached above 98% and production stopped, with a total gas production of approximately 2,864.34 L (**Table 4**).

The experimental results of the Model 2 continuous packer water control process showed essentially no change in the bottom water cone inlet characteristics before water was seen. It was still a central cone inlet. After water emergence, the overlying gravel rapidly sealed the water emergence location, and the other horizontal sections continued to produce. The gas–water

TABLE 4 | Quantitative comparison statistics of simulation results from different models.

	Waterless gas extraction period		Total gas production time		Total gas production	
	See water time/d	Extension rate/%	Total production time/d	Extension rate/%	Total gas production/L	Growth rate/%
Model 1	13.684	—	14.692	—	2,864.34	—
Model 2	13.693	—	16.497	12.29	3,035.05	5.96
Model 3	15.273	11.61	17.007	15.76	3,258.19	13.75

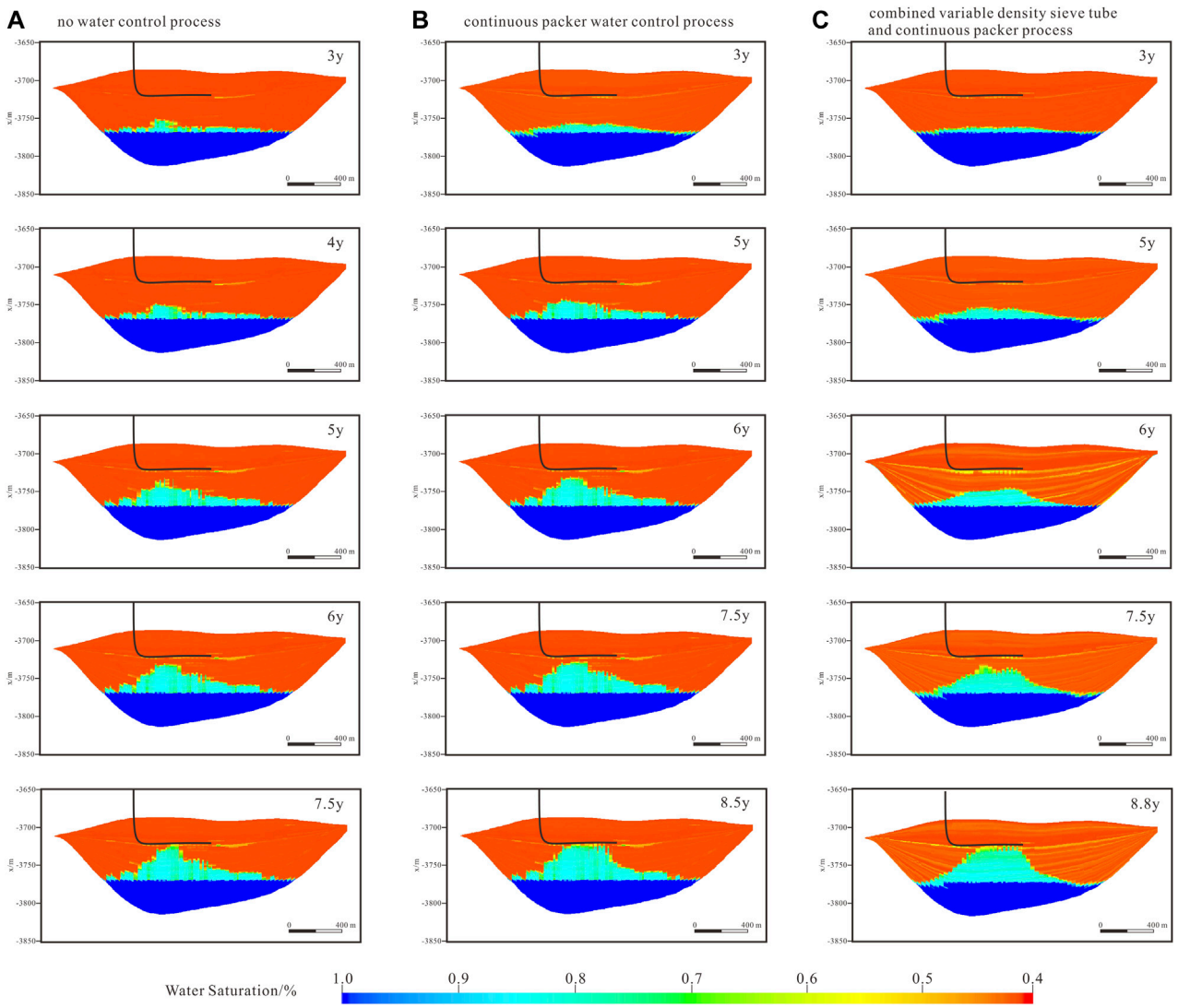

FIGURE 6 | Diagram of the water intrusion process in well H1 for different water control models. **(A)** No water control process. **(B)** Continuous packer water control process. **(C)** Combined variable density sieve tube and continuous packer process.

interface began to migrate laterally along the horizontal section from the water spot (**Figure 5B**). When the horizontal section was fully producing water, the gas–water interface profile features were parallel to the horizontal section. Model 2 showed water at 13.693 days of production, approximately 13 min longer than Model 1. Consideration was given to the laying of the overlying gravel, error between models, and total production time. The time difference between the two models was ignored in the later analysis. The time to water was considered to be in approximate agreement. The total gas production time for

TABLE 5 | Quantitative comparison statistics of simulation results from different models.

	Waterless gas extraction period		Total gas production time		Total gas production	
	Time to see water/year	Extension rate/%	Total production time/year	Extension rate/%	Total gas production/10^8 m^3	Growth rate/%
Model 1	7.1	—	7.5	—	13.42	—
Model 2	8.0	12.67	8.8	17.33	15.47	15.27

Model 2 was approximately 16.497 days, and the total gas production was approximately 3,035.05 L. The gas production time was approximately 12.29% longer, and the total gas production was approximately 5.96% higher than that of Model 1 (**Table 4**).

The combined water control process of Model 3 demonstrated a balanced bottom water cone inlet interface during gas production. It made it more homogenous, and after seeing water, the location of the water is effectively blocked without affecting the continued production of other horizontal sections (**Figure 5C**). Therefore, it had better water control effect. Model 3 saw water at an extension rate of approximately 11.61% compared with Models 1 and 2. The total production time was extended by 15.76% compared with the no water control condition, extending to 17.007 days. The total gas production was 3,258.19 L, with a gas production growth rate of approximately 13.75% compared with the no water control condition (**Table 4**).

Model 2 is a water control process with a combination of a variable density screen tube and a continuous packer. Due to the lateral flow stopping capacity of the continuous packer for the gas, the mutual interference of gas production in each section is reduced and radial seepage is dominant. The percolation rate is related to reservoir inhomogeneity and sieve tube density (**Figure 6B**). Therefore, based on the basic design of the model, the bottom water below the horizontal section is characterized by a more gentle morphology of the gas–water interface profile during the cone advance. Initially, the main feature is an overall uplift, with a "double-peaked" structure around 7.5 years of production but still with a gentle overall profile. Water starts to appear after 8.0 years of production and ceases after 0.8 years of production. This is 0.9 years later than the time taken by Model 1 and represents an extension of time of approximately 12.67%. Total gas production was 15.47 × 10^8 m^3, with a gas production growth rate of approximately 15.27% of that under uncontrolled water conditions (Tab 5).

NUMERICAL SIMULATION EXPERIMENTAL ANALYSIS

Numerical Model Design

Numerical simulations of the combined water control process model were carried out to validate the physical simulations against each other (**Figure 6**). The radial resistance of the laminated particles before they see water is very small and it hardly affects the flow of the fluid. In contrast, the resistance to axial flow is large, about 10^4 times the resistance to radial seepage (Wan et al., 2020). Therefore, in the model setup with lamella-sealed particles, the axial permeability of the particle-filled annulus is equivalently reduced by a factor of 10^4. The radial permeability parameter is not changed so that no lateral fugitive flow occurs during gas production.

Numerical Simulation Results

The results of Model 1 show that the H1 well, without the implementation of a water control process, began to lift the initial bottom water as a whole upward as production progressed. The bottom water starts to cone in at the middle of the horizontal section. After 7.1 years of production, the bottom water tapered into the horizontal section and started to produce water (**Figure 6A**). Due to the high reservoir pressure, the bottom water multiplier was high. The horizontal section floods rapidly after water production. Water production rises in a near-linear fashion in the short term (approximately 0.4 years). When the gas production time is 7.5 years, the horizontal well section is completely filled with water. Total gas production was 13.42 × 10^8 m^3 (**Table 5**).

DISCUSSION

The physical and numerical simulations carried out in this study for the continuous packer and its combined water control process with the variable density screen tube yielded consistent results. The results of the two simulation methods, Model 2 and Model 3, for both water control processes were within 10% error in the water-free recovery period, total gas production time, and total gas production volume (**Table 6**). Both the continuous containment and composite water control processes achieved considerable production enhancement.

A comparison of the simulation results for both physical and numerical simulations, Model 1 and Model 2, shows that the continuous packer is predominantly water-seeking and water-blocking. The total production time of the process pair with the horizontal well is effectively extended, and the rate of water production is significantly reduced, indicating that the continuous packer has a high water-stopping capacity. Although able to directly stop the bottom water from entering the horizontal section at the-water-seeing location, it does not affect the normal production of gas at other locations in the horizontal section. The gas permeable water blocking effect is more consistent with the physical simulation results recognized (Liu et al., 2020). The process belongs to the late extraction water blocking measures and the main advantages are as follows: 1) no need to find water operation; 2) the whole well section is set up to prevent adaptive water blocking and solve the problem of out-of-tube fugitive flow; 3) once blocking water, there is no need to worry about the problem of extra increase of water outlet point later, and long-term effective; 4) gravel filling has good anti-

TABLE 6 | Comparison of error statistics between physical and numerical simulation results.

Extension of the water-free gas extraction period/%			Total gas production time extension rate/%			Total gas production extension/%		
Physical simulation	Numerical simulation	Error	Physical simulation	Numerical simulation	Error	Physical simulation	Numerical simulation	Error
11.61	12.67	8.37	15.76	17.33	9.06	13.75	15.27	9.95

sand effect. However, there are still certain shortcomings for water control operations, that is, the failure to change the bottom water cone in speed or form. The simulation results of the water control model with the combination of the continuous packer and variable density screen tube solved the abovementioned problems well. The resistance to percolation in the axial direction of the laminated packer particles reduces the out-of-tube fugitive flow. The gas percolation rate at each location in the horizontal section is controlled mainly by the reservoir properties. This, combined with the variable density distribution of the orifice of the screen tube, matches the inhomogeneity of the reservoir. The gas percolation rate is balanced across the horizontal section. The gas–water interface during bottom water ascent in Model 3 has a greater extensional width (along the horizontal production section). The bottom water beneath the entire horizontal section has a smoother gas–water interface during ascent. This ensures efficient and long-term production of the horizontal well.

In terms of physical model design, this is influenced by factors such as size of the kettle itself, ratio of the kettle to the horizontal section, reservoir pore and seepage conditions, and inhomogeneous characteristics. It is not possible to avoid an exact match between the physical model and the relevant parameters or ratios of the actual gas reservoir and its production process. Based on the similarity principle (Shen et al., 2013), it can show the ability of bottom water coning upward under different permeability conditions according to the gas production capacity and pressure drop characteristics of different positions in the horizontal section and complete the characterization of the bottom water coning process. Of course, it is affected by the degree of reservoir inhomogeneity. The absolute flatness of the gas–water interface cannot be satisfied (Wang et al., 2012). In this experiment, due to the large coefficient of variation between sections, the gas–water interface appears to have a "waveform" structure during ascent. Therefore, the best water control effect of the combination of continuous packer and variable density screen tube requires a low degree of reservoir inhomogeneity. When the gas–water interface reaches the horizontal section, the clad packer particles continue to produce the same water control effect as in Model 2. This further enhances the production time after water is seen. However, due to the larger width and gentler morphology of the air–water interface below the horizontal section in Model 3, the initial contact with the horizontal section at the onset of water is extensive, resulting in insufficient ability to extend the total gas production time after the onset of water.

CONCLUSION

1) Numerical and physical simulation studies and comparative analyses were carried out based on production well data from the LS 25–1 gas field. We found that a single water control technique has limited effectiveness in controlling water in deepwater gas reservoirs. A combination of multiple water control techniques is required to achieve the desired results.
2) The results of the study also demonstrate the advantages of the continuous containment water control process for deepwater gas reservoirs. The water control principle is applicable to deepwater gas reservoirs. When a horizontal well starts producing water, no other measures are required to locate the location of the water produced. It is then possible to effectively reduce the amount of water produced at that location. Rapid water flooding of the horizontal well is prevented, thereby ensuring that the horizontal section continues to produce gas at locations where no water was produced.
3) The combination of the continuous packer and variable density screen tube can maximize the water control effect of both processes. It can greatly enhance the recovery rate of the producing wells. At the early stage of gas reservoir production, the overlaid packer particles can greatly reduce the water tampering effect in the annulus of the horizontal section. The radial percolation rate of gas at each location in the horizontal section is consistent with the inhomogeneity of the reservoir, ensuring that the gas production rate in each section of the horizontal well matches the density of the screen tube borehole and slows the bottom water cone in and balancing the gas–water interface during production. After water is seen, the overburden sealing particles continue to prevent bottom water from entering the horizontal section and causing flooding.

DATA AVAILABILITY STATEMENT

The data used to support the findings of this study are available from the corresponding author upon request.

AUTHOR CONTRIBUTIONS

DW: conceptualization; YL: methodology; LM: validation; FY: formal analysis; SL: investigation; YQ: writing the original draft; SJ: writing— review and editing.

ACKNOWLEDGMENTS

The authors are grateful for the Hainan province major Science and Technology Project (ZDKJ2021025), Heilongjiang Province

Key Research and Development project (GZ20210015), Heilongjiang Province Joint Guide Fund project (LH2021E017), Northeast Petroleum University start up funding project for talent introduction and scientific (1305021856), and College of Petroleum Engineering excellent scientific research talent cultivation project (15041260507). We thank Sun Zaixing for his comments and suggestions in the writing of this paper.

REFERENCES

Chen, K., Yang, X. B., Li, M., Li, A. Q., Wang, Z. Z., Li, F. X., et al. (2020). Research and Application Effectiveness of Target Search Technology System in the deepwater Exploration Mature Area of Qiongdongnan Basin. *China Offshore Oil and Gas.* 32 (3), 33–42. *(In Chinese)*. doi:10.11935/j.issn.1673-1506.2020.03.004

Irani, M., Bashtani, F., and Kantzas, A. (2021). Control of Gas Cresting/coning in Horizontal wells with Tubing-Deployed Inflow Control Devices. *Fuel.* 293, 120328. doi:10.1016/j.fuel.2021.120328

Li, H., Chen, D. C., and Meng, H. X. (2010). Optimized Design Model for Horizontal wells with Variable Density Injection. *Pet. Exploration Development.* 37 (3), 363–368. *(In Chinese)*. doi:10.1016/S1872-5813(11)60005-4

Liu, Y. K., Wang, H. D., Meng, W. B., Zhang, C., Zhi, J. Q., and Shen, A. Q. (2020). Experiments on Production Enhancement of Horizontal Wells Filled With Gas Reservoirs With Gas-Permeable Water-Barrier Gravels in Deep Subsea Water Reservoirs. *Nat. Gas Industry.* 40 (1), 61–68. *(In Chinese)*. doi:10.3787/j.issn.1000-0976.2020.01.008

Pang, W., Chen, D. C., Zhang, Z. P., Jiang, L. F., Li, C. H., Zhao, X., et al. (2012). Optimization Model for Segmented Variable Density Injection of Horizontal Wells in Non-Homogeneous Reservoirs. *Pet. Exploration Development.* 39 (2), 214–221. *(In Chinese)*. doi:10.1016/s1876-3804(12)60036-6

Rao, F. P., Dong, Y. L., Wu, J. S., Qi, Y. K., Tang, Q., and Wang, X. B. (2010). Water Control Completion Process for Horizontal Wells in Bottom Water Reservoirs in Dagang Oilfield. *Pet. Drilling Technology.* 32 (3), 107–109. *(In Chinese)*. doi:10.13639/j.odpt.2010.03.025

Shen, W. J., Li, X. Z., Lu, J. L., and Liu, X. H. (2013). Similar Theoretical Study on Physical Simulation of Anomalous High-Pressure Gas Reservoir Development. *Sci. Technology Eng.* 13 (35), 10460–10465. *(In Chinese)*. doi:10.1006/j.issn.2013.09.13

Shi, Y. (2015). China's First deepwater High-Temperature and High-Pressure Exploratory Well Completed in South China Sea. *Oil Drilling Prod. Technology* 37 (5), 45. *(In Chinese)*.

Sun, K., Guo, B. Y., and Saputelli, S. (2011). Multinode Intelligent-Well Technology for Active Inflow Control in Horizontal Wells. *SPE Drilling and Completion.* 26 (3), 386–395. doi:10.2118/130490-pa

Sun, X. D., and Bai, B. J. (2017). Status of Research on Water Control Technology in Horizontal wells at home and Abroad. *Pet. Exploration Development* 44 (6), 967–973. *(In Chinese)*. doi:10.1016/s1876-3804(17)30115-5

Wan, X. J., Wu, S. W., Zhou, H. Y., Yuan, H., and Song, L. Z. (2020). Research and Experiments on Water Control Technology of Flow-Controlled Screen Tube With Particle Filling. *Drilling Prod. Technology.* 43 (5), 61–63. *(In Chinese)*. doi:10.3969/J.ISSN.1006-768X.2020.05.17

Wang, H. J., Xue, S. F., and Gao, C. F. (2012). Methodology of Variable-Density Hole-Shot Profiling in Horizontal wells. *Oil Gas Geology. Recovery.* 19 (6), 87–90. *(In Chinese)*. doi:10.13673/j.cnki.cn37-1359/te.2012.06.022

Wang, P. M., Luo, J. H., Bai, F. L., Yang, J. B., and Bu, R. Y. (2001). Research Progress on Water Plugging Technology for Gas Wells at Home and Abroad. *Drilling Prod. Technology.* 24 (4), 28–30. *(In Chinese)*. doi:10.3969/j.issn.1006-768X.2001.04.008

Wang, Q., Liu, E., Zhang, H. L., and Zheng, J. P. (2011). Preferred Model for Flow and Water Control Sieve Pipe in Coupled Horizontal wells in Oil Reservoirs. *Acta Petrolei Sinica.* 32 (2), 346–349. *(In Chinese)*. doi:10.7623/syxb201102026

Wei, J. G., Wang, Z. M., and Wang, S. Q. (2009). Segmental Optimization Model for Injection Parameters of Horizontal Wells in Non-Homogeneous Reservoirs. *J. China Univ. Pet. (Natural Sci. Edition).* 33 (2), 75–79. *(In Chinese)*. doi:10.3321/j.issn:1673-5005.2009.02.014

Xu, J., Wu, K., Li, R., Li, Z., Li, J., Xu, Q., et al. (2018). Real Gas Transport in Shale Matrix With Fractal Structures. *Fuel* 219, 353–363.

Xu, J., Wu, K., Li, R., Li, Z., Li, J., Xu, Q., et al. (2019). Nanoscale Pore Size Distribution Effects on Gas Production from Fractal Shale Rocks. *Fractals* 27 (8), 1950142.

Xu, J., Chen, Z., and Li, R. (2020). Impacts of Pore Size Distribution on Gas Injection in Intraformational Water Zones in Oil Sands Reservoirs. *Oil Gas Sci. Technol.* 75 (6), 75.

Xu, X., Li, X., Hu, Y., Mei, Q., Shi, Y., and Jiao, C. (2021). Physical Simulation for Water Invasion and Water Control Optimization in Water Drive Gas Reservoirs. *Sci. Rep.* 11, 6301. doi:10.1038/s41598-021-85548-0

Yan, H. T., Xu, W. J., Jiang, W. D., and Zou, X. B. (2021). Adaptive Water Control Technology for Horizontal Wells in Offshore Bottom Water Reservoirs. *Pet. Geology. Oilfield Development Daqing.* 40 (3), 71–76. *(In Chinese)*. doi:10.19597/j.issn.1000-3754.202009019

Zeng, C., Duan, Y. G., and Liu, Y. F. (2014). The Role of Downhole Inflow Controller in Water Control and Dissection in Horizontal Wells in Bottom Water Reservoirs. *Drilling Prod. Technology.* 37 (3), 67–70. *(In Chinese)*. doi:10.3969/J.ISSN.1006-768X.2014.03.20

Zhang, J. B., An, Y. S., Wang, H. L., Xiong, M. S., and Li, Q. Q. (2021). Numerical Simulation Method for the Production Dynamics of ICD Completions in Horizontal Wells with Continuous Packers. *China Offshore Oil and Gas.* 33 (3), 121–125. *(In Chinese)*. doi:10.11935/j.issn.1673—1506.2021.03.014

Zhao, Y., Yang, H. B., and He, S. R. (2012). Flow Control Completion Technology for Horizontal Wells With Screen Tubing in the Shengli Low-Permeability Oilfield. *Pet. Drilling Tech.* 40 (3), 18–22. *(In Chinese)*. doi:10.3969/j.issn.1001-0890.2012.03.004

Zhou, S. T. (2007). Optimization Analysis of Borehole Density in Shot-Hole Horizontal wells. *Pet. Drilling Tech.* 35 (5), 55–57. *(In Chinese)*. doi:10.3969/j.issn.1001-0890.2007.05.016

Conflict of Interest: FY was employed by Bohai Oilfield Research Institute of CNOOC Ltd.

The remaining authors declare that the research was conducted in the absence of any commercial or financial relationships that could be construed as a potential conflict of interest.

Publisher's Note: All claims expressed in this article are solely those of the authors and do not necessarily represent those of their affiliated organizations, or those of the publisher, the editors, and the reviewers. Any product that may be evaluated in this article, or claim that may be made by its manufacturer, is not guaranteed or endorsed by the publisher.